

Comparison of the virtual biopsies of a nodular basal cell carcinoma and an actinic keratosis: morphological, cellular and collagen analyses

Abstract

Previous literature reports suggest that tissue stiffness is a predictor of cancer and metastatic behavior. We have used optical coherence tomography and vibrational analysis (VOCT) to characterize normal skin, scar, a basal cell carcinoma and an actinic keratosis non-invasively and non-destructively.

It is concluded that enhanced VOCT images of surface roughness and lesion morphology in combination with estimates of cellular and collagen content may assist the clinician in better characterizing different skin lesions prior to excision. The use of VOCT in the physician's office will assist the surgeon in preoperative planning and facilitate patient treatment that will benefit both the doctor and patient.

Keywords: basal cell carcinoma, actinic keratosis, optical coherence tomography, vibrational optical coherence tomography, mechanical properties, stiffness, modulus, collagen, extracellular matrix, keratinocytes

Volume 5 Issue 2 - 2019

Frederick H Silver,¹ Ruchit G Shah,² Michael Richard,³ Dominick Benedetto⁴

¹Department of Pathology and Laboratory Medicine, Robert Wood Johnson Medical School, Rutgers, The State University of New Jersey, USA

²Graduate Program in Biomedical Engineering, The State University of New Jersey, USA

³Neigel Center for Cosmetic and Laser Surgery, USA

⁴Center for Advanced Eye Care, USA

Correspondence: Frederick H Silver, Department of Pathology and Laboratory Medicine, Robert Wood Johnson Medical School, Rutgers, The State University of New Jersey, Piscataway, NJ 08854, USA,
Email silverfr@rutgers.edu, fhsilver@hotmail.com

Received: April 24, 2019 | **Published:** May 06, 2019

Abbreviations: OCT, optical coherence tomography; VOCT, vibrational optical coherence tomography; ECM, extracellular matrix; BCC, basal cell carcinoma; AK, actinic keratosis; SCC, squamous cell carcinoma; NMSC, non-melanoma skin cancer

Introduction

In 2014, an estimated 5 million people in the USA were treated for skin cancer at a cost of 8.1 billion dollars.¹ The number of US citizens developing skin cancer in the future and the associated costs of treatment are expected to dramatically increase as the number of US citizens in the 55 to 85-year-old age group increases. The number of people in the US between the ages of 55 and 85 years old is expected to increase to 125 M by 2050 and about 20% of this group will have a skin cancer before the age of 70.¹ Identification of tissue biomechanical markers like tissue stiffness in conjunction with enhanced imaging can be used to non-invasively screen patients for skin cancer. This would facilitate detection and early removal.

Increased tissue stiffness (also termed modulus) has been shown to be a characteristic of potential tumor metastasis² and is the result of the abnormal deposition of collagen fibers, the major component of extracellular matrix (ECM). This leads to altered tissue biomechanical properties of the skin. The orientation and amount of collagen in skin lesions reflects tissue metabolism and may be used to characterize tissue lesions.³ Skin cancer is a heterogeneous group of lesions comprising cutaneous melanomas and non-melanomas (NMSC).⁴ The NMSCs refer to keratinocyte carcinomas, including basal cell carcinomas (BCC), squamous cell carcinomas (SCC) and actinic keratosis (AK).⁵

BCC is a cutaneous malignant proliferation of cells that is thought to derive from the basal layer and outer root sheath of hair follicles.⁴ The nodular type consists of aggregates of basaloid cells with well-defined borders, a peripheral palisading of cells, and a typical cleft.⁴ Mitotic activity is not normally present but can be present in aggressive forms of the lesion. BCC is the most common human cancer and it is usually caused by excessive exposure to ultraviolet light.⁶

In comparison, AK is thought to be an early form of SCC. It is characterized as a horizontal alteration of parakeratotic and/or keratotic hyperkeratosis with an atrophic epidermis.⁶ Neoplastic keratinocytes in the basal layer show increased cellularity, nuclear pleomorphism and scattered mitoses. Both nodular BCC and AK are characterized by hypercellularity of the epidermis; however, it is unclear whether alteration of the organization and amounts of collagen in the papillary dermis occur in these lesions.

Reported values of the stiffness of tumors and cancer cells differ for normal and cancerous lesions.⁷⁻⁹ For most breast and colorectal cancer cell types, the stiffness of neoplastic tumors is reported to increase compared to that of neighboring normal tissue,⁴⁻⁶ while in contrast, cancer cells, irrespective of the carcinoma, are reported to usually be softer than their normal counterparts.^{10,11} However; the later studies may not consider cell-cell interactions that would increase cellular stiffness. The measurement of the stiffness of cells and extracellular matrices non-invasively *in vivo* would be a useful parameter to correlate with the histopathology of cancerous lesions.

We have developed a technique to combine optical coherence tomography (OCT) with vibrational analysis to image and analyze the biomechanical properties of tissues non-invasively and non-

destructively. The result of this analysis is a “virtual biopsy” of skin.^{12–18} These measurements along with *in vitro* calibration data can be used to interpret mechanical measurements made *in vivo*.^{12–18} By combining tissue biomechanical data with imaging, lesion margins and types can be characterized prior to surgical excision of suspected malignant skin lesions. In addition, a comparison of the structure and stiffness of lesions such as nodular BCC and AK can be used to characterize the differences between these two lesion types.

Methods

In Vitro Calibration curve construction using measurements on extracellular matrices (ECMs)

Vibrational optical coherence tomography (VOCT) is a new technique developed in the Department of Pathology at Robert Wood Johnson Medical School, Rutgers University. It uses near infra-red light and audible sound to image and measure the resonant frequency of tissues.^{12–19} The resonant frequency of tissue is directly related to the tissue stiffness as described previously.^{12–19}

A calibration curve of modulus values for control ECMs was constructed by comparing moduli measured using conventional tensile testing and vibrational OCT measurements *in vitro* as previously described.^{12–19} The calibration curve indicated a roughly one-to-one relationship between tensile moduli and vibrational moduli measured on the same samples including the decellularized human dermis, pig skin, and bovine cartilage.^{12–19}

The resonant frequency, f_r , is related to the modulus, E , by equation (1)

$$E = m(2\pi f_r)^2 \left(\frac{L}{A} \right) \quad (1)$$

where m , L and A are the sample mass, length and cross-sectional area. The resonant frequency was determined after correction for the resonant frequencies exhibited by the speaker, sample holders and any interference due to line voltage fluctuations.^{12–19}

Vibrational OCT measurements

Image collection

OCT cross-sectional images were obtained using an OQ Labscope (Lummedica Inc., Durham, NC) and a laboratory spectral-domain optical coherence tomography device (SD-OCT) operating in the scanning mode.^{12–19}

OCT and vibrational analysis *In Vivo*

Transverse sample displacement was generated by placing a speaker next to the skin or under the excised lesion to be studied by spectral-domain optical coherence tomography (SD-OCT), a non-contact, interferometric technique as discussed previously.^{9–15} The SD-OCT system uses a fiber-coupled superluminescent diode light source with an 810 to 1325 center wavelength and 100 nm bandwidth (full-width at half maximum) as described previously.^{12–19}

In vivo studies on the mechanical properties of skin and healed scar tissue were conducted by hard wiring a 24 mm x 14 mm rectangular speaker (Digi-Key, Thief River Falls, MN) to a Samsung cell phone. A frequency generating app was downloaded from the Google Play Store onto the cell phone. This app was capable of driving the speaker

between 10 and 20,000 Hz. The speaker was applied to the skin using surgical tape and it was used to generate a sinusoidal sound wave that vibrated the skin. During *in vivo* measurements, no sensation of the light or sound impinging on the skin was felt. The sound intensity was inaudible unless the speaker was placed near the subject’s ear to make sure it was energized. *In vitro* measurements on an excised BCC and AK lesions were made by placing each lesion on a glass slide and mounting the glass slide on a plastic support under which a speaker was placed to vibrate the tissue as discussed previously.^{18,19}

The resonant frequency of each sample was initially estimated by measuring the transverse displacement resulting from sinusoidal driving frequencies ranging from 30 Hz to 500 Hz, in steps of 50 Hz. Once the region where the maximum frequency was identified, smaller steps of 10 Hz were used to more accurately identify the peak frequency and the actual resonant frequency, f_r . The stiffness (modulus) of skin and the skin lesion were calculated from measurements of the resonant frequency and tissue thickness made using VOCT and images of the tissues. Moduli were obtained from a calibration curve that relates resonant frequency and thickness to modulus values (Figure 1).

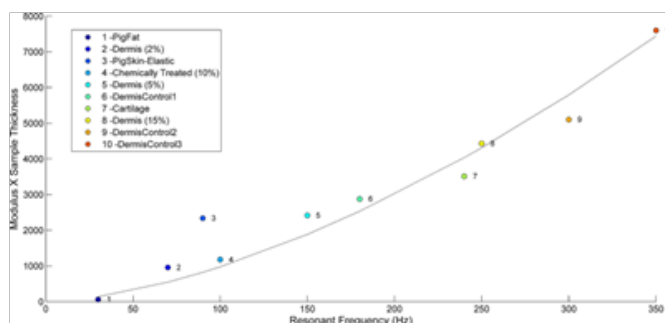


Figure 1 Calibration curve of tissue modulus times thickness versus resonant frequency for different extracellular matrices. This figure was modified from reference.¹⁴ Note the modulus for cellular materials (fat and Staph Aureus) is lower (less than 0.1 MPa) than for normal dermal collagen (2 to 3 MPa) and scar tissue (7 MPa).

The original grayscale OCT images of skin, scar and skin lesions were pseudo-color-coded based on the pixel intensities to provide better images of the tissue components. The enhanced OCT images used darker colored (blue and purple) regions to reflect lower pixel intensities while the lighter (yellowish) regions reflected higher pixel intensity regions.

Results

OCT images of scar tissue are different than that of normal skin; scar tissue appears to have a “smoother” surface than normal skin as reported previously.^{17,18} The epidermis is quite thin in both normal skin and scar tissue and the cellular layers in the epidermis are more visible by color coding the image based on pixel density as shown in Figure 2. The stratum corneum, spinosum and basale, and collagen of the papillary dermis are labeled A, B, and C, respectively in the enhanced OCT image. A plot of weighted displacement versus frequency for normal skin and scar tissue is shown in Figure 3. Note the resonant frequency of scar tissue is much higher than that of normal skin *in vivo*.

The resonant frequency values obtained from *in vivo* studies were corrected for differences in tissue thickness using the calibration

curve for ECMs shown in Figure 1 to calculate values of the moduli. Plots of weighted displacement for skin and scar show peaks at 90-100 Hz (normal skin) and 220 to 230 Hz (scar tissue), respectively and the calculated moduli are about 2.0 to 3.0 MPa (skin) and 7.0 MPa (scar) (Table 1). Note the resonant frequencies of the epidermis of skin and scar tissue are not measurable since the epidermis is too thin to generate a signal.

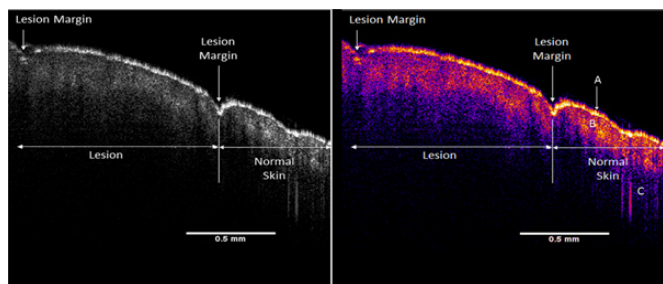


Figure 2 OCT image of normal human skin and scar. The interface between scar tissue and normal skin is marked by a surface depression and a difference in the height of the hills and valleys seen by OCT. Normal skin has more apparent hills and valleys in the surface layer than scar tissue. The interface between normal and scar tissue is marked in the figure by the arrows. The stratum corneum in both normal skin and healed scar tissue is very thin. Additional OCT images of normal skin and scar are shown in reference [14] illustrating the number of larger hills and valleys that are seen in normal skin when compared to scar tissue. The stratum corneum, spinosum and basale, and collagen of the papillary dermis are labeled A, B, and C, respectively in the enhanced OCT image.

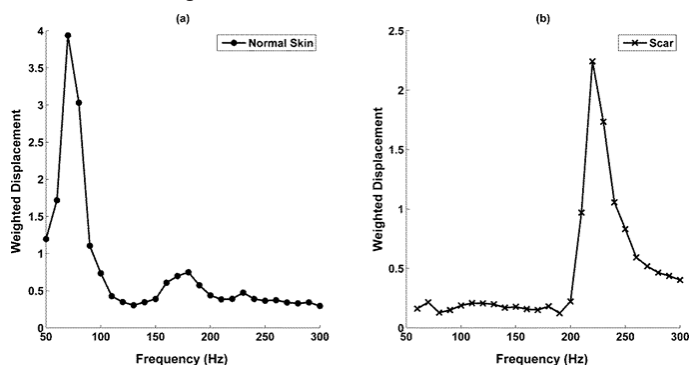


Figure 3 Weighted displacement versus frequency for normal skin and scar tissue. Note the resonance frequency of normal skin is 90 to 100 Hz depending on the tissue thickness whereas that for scar tissue is 220-230 Hz.

Table 1 Resonant Frequencies and Moduli Values of Normal Skin, Scar, Fat and Verrucous Carcinoma from references 14, 16 and Basal Cell Carcinoma and Actinic Keratosis

Tissue	Resonant Frequencies (Hz)	Modulus #1 (MPa)	Modulus #2 (MPa)
Skin	90-100	None	2.0 to 3.0
Scar	220-230	None	7
Fat	40	0.03	None
Staph Aureus	40	0.056	None
Verrucous C	50, 150-170	0.686	2.57
Actinic K	70, 140-180	0.89	3.05
Basal CC	60, 160	0.618	2.66

The OCT and enhanced color-coded images of skin and scar are shown in Figure 2. Note the thin epidermis (A) shown in yellow on both the normal skin and scar (Figure 2). This layer appears to be the stratum corneum. Below the yellow layer in the enhanced OCT image of the normal skin and scar one sees a discontinuous pinkish layer of cellular material (B). This layer appears to be a composite of the stratum spinosum and stratum basale. Finally, the dark blue region (C) of the enhanced OCT image is composed largely of the collagen fibers found in the papillary dermis (C).

A gross image of excised BCC and AK lesions are shown in Figure 4; the width of both lesions is about 3 mm. The lesions were removed from an eyelid, placed on a glass slide and studied immediately with VOCT before they were sent out for histopathology. The OCT and enhanced VOCT images of the lesions are shown in Figures 5-7 along with the H&E stained tissue sections of the lesions (Figures 6&7).



Figure 4 Gross images of BCC (left) and AK (right) lesions. Note the small size of the lesions which may result in the introduction of processing artifacts into the sections viewed for histopathological analysis.

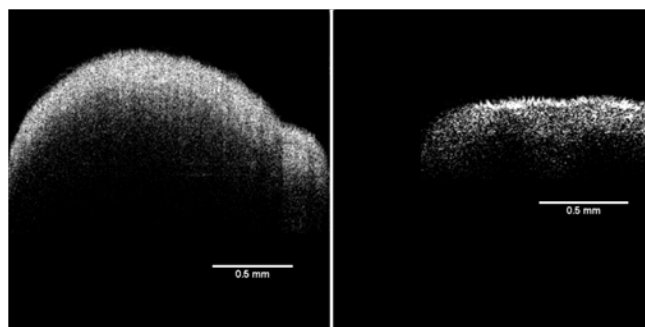


Figure 5 OCT images of BCC (left) and AK lesion (right).

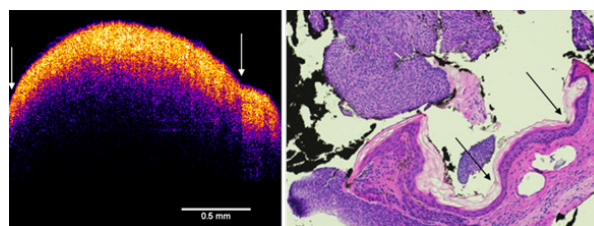


Figure 6 Enhanced OCT image of BCC (left) and H&E stained tissue cross-section of a BCC lesion (right). Note the arrows showing the small cleft between the two fragments of the lesion (left) and the detached portion of the lesion in the H&E stained section (right). The nodule seen in the histological section is composed of basal cells. The top of the enhanced OCT image shows a thin blue layer that is equivalent to the dead squamous layer sloughing off of the lesion in the tissue section. The yellow-pink layer (left) is equivalent to the basal cell layer (right). Note the increased thickness of the epidermis as compared to normal skin and scar (Figure 2).

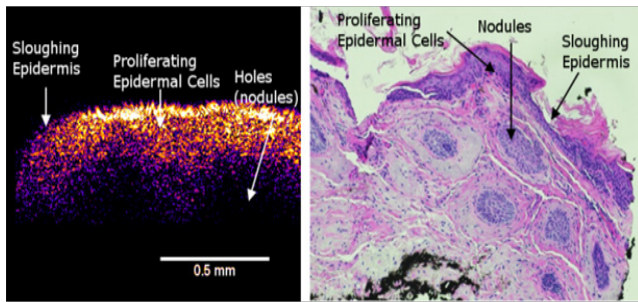


Figure 7 Enhanced OCT image of an AK lesion (left) and an H&E tissue cross-section (right). Note the thin blue layer on the surface of the enhanced OCT image (left). This is equivalent to the epidermis sloughing off in the H&E section (right). The thickened yellow-pink epidermal layer (left) is seen to have holes that are seen as nodules in the H&E stained section (right).

In the enhanced OCT image of the basal cell carcinoma, the thin blue surface layer appears to correspond with the layer of dead keratinocytes seen in the tissue section. The pinkish yellow layer below the stratum corneum appears to be the layer of proliferating basal cells that appears to be discontinuous at the interface with a large nodule (Figure 6) that appeared to be separated from the lesion during processing for histopathology (Figure 6). The lesion is broken

and appears discontinuous. The histopathology of the lesion is confused by what appears to artifacts that occur when the lesion is cut and embedded since it is almost continuous in the VOCT image except what appears to be a small cleft (Figure 6).

In the enhanced OCT image of the AK, the blue layer appears to correspond to a thin layer of dead keratinocytes. The yellow-pinkish layer corresponds to a thickened layer of epidermal cells compared to normal skin (Figure 2). This layer appears to be composed of the proliferating basal cells and the round areas seen as holes in the image (Figure 7) corresponds to the round nodules in the histopathology (Figure 7). The bluish layers below and around holes in the left part of Figure 7 appear to be the extracellular matrix of the papillary dermis.

A plot of weighted displacement versus frequency for the BCC and AK lesions is shown in Figure 8. Note the presence of peaks at 40-60 Hz and at 140-180 Hz which correspond to moduli of between 0.686 and 0.809 MPa and 2.57 and 3.05 MPa. The moduli associated with these peaks are listed in Table 1 along with moduli for normal skin, scar tissue and fat. Note the peak at approximately 150 Hz (collagen) for the BCC lesion is very small while that for the AK lesion is much higher. In contrast, the height of the peak at 40 Hz (cellular peak) for the BCC lesion is much higher than the peak for the AK lesion. Thus the BCC lesion is composed primarily of cells while that of the AK lesion has cells and collagen.

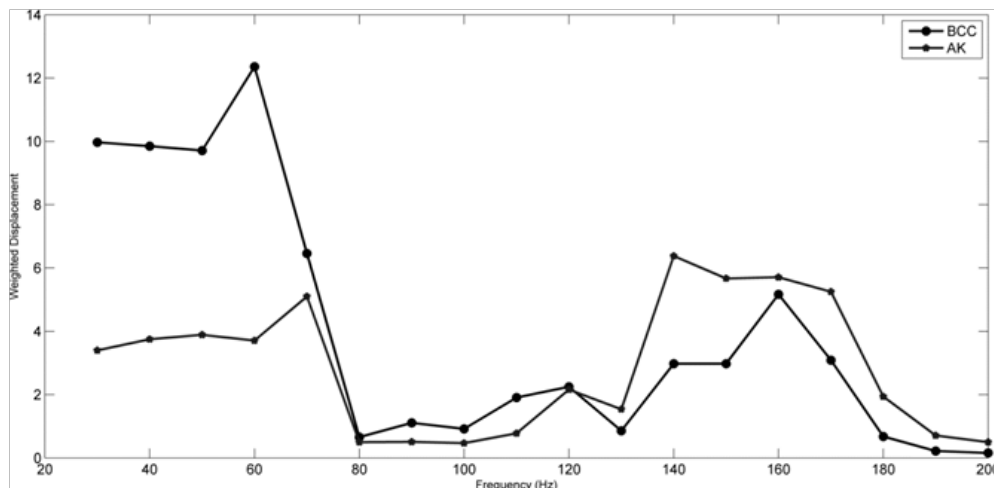


Figure 8 Weighted displacement versus frequency for BCC and AK lesions. Note the BCC lesion has a large cellular peak at about 60 Hz and a small peak at 160 Hz (collagen) while the AK lesion has similar size peaks at about 70 Hz and 140-170 (Hz) suggesting an approximately equal amount of cells and collagen. The BCC lesion is primarily composed of cells with small amounts of collagen.

Discussion

While most clinicians can visually identify many lesion types, studies demonstrate only a 98% concordance rate between the pre-operative and post-operative determination of malignancy. Also, there is no one clinical growth pattern that has been demonstrated to be definitively associated with benign lesions.²⁰ Normally, lesion depth or margins can't be defined without performing a surgical excision and waiting for frozen sections. The time between surgical excision and the pathologic results may be as great as 60 minutes for a frozen section. During this time patients await verification of complete lesion excision before wound closure. The preoperative clinical assessment of the extent of a tumor in three dimensions would facilitate surgical

planning and allow dermatologists to know which tumors are deep enough to require a referral to a Mohs specialist.¹⁸ With improved preoperative imaging and measurement of tissue properties, micrographic surgery, as well as surgical removal and identification of other skin lesions, could be facilitated, made more cost-effective and be less time-consuming for patients and surgeons.¹⁸

From 1996 until 2013 Mohs surgical procedures to remove skin cancers increased 469%.¹ Basal cell and squamous cell carcinomas affect more than 1 million individuals in the US each year while the diagnosis of non-melanoma skin cancer accounts for about 3.5 million new cases in the US each year.¹ The chances of getting skin cancer by the age of 70 are one in five making the population at risk to be about 25 M people by 2050.¹

We have developed a non-invasive and non-destructive test, vibrational optical coherence tomography (VOCT), to image and measure the stiffness of skin lesions.¹⁷⁻¹⁹ This technique can be used to measure the stiffness of any substance by vibrating the material and measuring its resonant frequency.¹²⁻¹⁹ Since tissue stiffness has been identified as a marker for cancerous lesions and as a predictor of metastatic behavior,² this technique would be useful in rapid identification of skin lesions. In addition, since the resonant frequency of the epidermis of normal skin and scar tissue cannot be measured, due to the thinness of the normal epidermis, this technique would be useful in identifying pathological changes to both the epidermis and dermis. Any cellular proliferation of the epidermis or fibrosis of the dermis could be measured by performing a virtual biopsy of tissue using infra-red light and audible sound that is the basis of VOCT.

In this paper, we present data on the use of VOCT for performing a virtual biopsy on normal skin, scar and BCC and AK lesions. Virtual biopsies of normal skin and scar have recently been reported and indicate that using this technique images of the epidermis clearly show details of groups of cells; however, the epidermis is too thin in normal skin and scar to accurately measure the stiffness.¹⁷⁻¹⁹ In this study, we report that enhanced OCT images of the epidermis and dermis clearly show differences in the thickness and morphology of normal skin, scar and BCC and AK. It is seen after examining the BCC, that both BCC and AK have decreased surface roughness that is more like a scar than wavy normal skin. The roughness of normal skin is seen using OCT and the period of the hills and valleys could be measured and tabulated as a function of age and location *in vivo*. Any changes in the surface roughness observed in both the epidermis and dermis may give information that may help to understand the pathogenesis of different skin disorders.

Both lesions have a thickened epidermis but the BCC has a large region that appears to be disconnected from the bulk of the carcinoma. AK is characterized by holes in the enhanced OCT image that correspond to the nodules seen by histopathology. Resonant frequency measurements suggest that the BCC lesion is made up of cells with resonant frequencies between 40 and 60 Hz. However, based on the ratio of low (40 to 60 Hz) and higher frequency peaks (140-160Hz) the collagen content of the BCC lesion is much smaller than the content of cells. The AK lesion has both cells and collagen in the papillary dermis based on the relative similar size of the low and high-frequency peaks. It may be possible to characterize the different variants of BCC and AK lesions by the ratio of the low and high-frequency peaks as well as the exact stiffness values found for each peak. It is anticipated that lesions with metastatic potential will show collagen stiffness that is more like scar tissue (7 MPa) than normal skin (2-3 MPa) since the former would reflect the need to rearrange the ECM around the cells to allow for cell migration.

The enhanced OCT images of the lesions compared to the histopathological images suggest that the tissue is modified during tissue processing, especially if the lesion is small and friable. Tissue processing can cause tissue shrinkage during fixation that can be as much as 30%.²¹ Cutting and sectioning can lead to fragmentation and dislocation of tissue components not seen with VOCT. The enhanced OCT images and resonant frequency data give a better idea of the relationship between the between cellular and collagenous components and may be useful in defining the extent, margins and depth of skin lesions prior to surgery and better define any remnants of the lesion after excision.

Refractive confocal microscopy (RCM) has been used to assist with microscopic evaluation of BCC lesions. RCM provides horizontal optical sections of skin at a nearly histological resolution.²² It is used to visualize enlarged blood vessels with very fast blood flow that characterize BCC.²² However, RCM like dermoscopy are solely imaging techniques and do not provide any quantitative data on blood flow or tissue stiffness. Vessel wall and tissue stiffness that can be measured using VOCT are reflective of blood flow rate and tissue composition. These are measurable quantities using VOCT and would provide complementary data to dermoscopy and RCM that are useful in the diagnosis of BCC.

The relationship between collagen orientation and the mechanical properties of extracellular matrices have been well established in the literature.²² Oriented collagen matrices exhibit higher moduli and lower strains to failure as compared to orientable collagen networks.³ The “apparent” increased stiffness of scar tissue is a result of the limited ability of scar tissue to stretch when an external load is applied.²³ Thus tissue stiffness is a measure of the collagen orientation in skin and skin lesions. Enhanced collagen orientation and increased collagen stiffness would be expected to be predictive of lesions that spread into other tissues as well as the movement of cancerous cells from the site of the initial lesion towards the surrounding blood vessels and lymph nodes required for metastasis. In this study, the collagen component appears to have a stiffness of about 2 to 3 MPa in both lesions and did not appear to change even though the amount of collagen was reduced in the BCC lesion as compared to the AK lesion.

Additional studies are needed with a variety of skin lesions to further characterize the relationship between the epidermis and papillary dermis based on the height and width of the cellular and collagen resonant frequency peaks. These data are needed to determine whether different lesions can be classified based on the OCT images and the changes in the resonant frequency when compared to normal skin. This would assist the surgeon in defining and characterizing different lesions prior to after excision of tissue. A skin lesion as small as 0.2 mm in diameter can be studied in patients using VOCT even before the lesion can be clearly seen by dermoscopy.

Conclusion

VOCT is a useful imaging technique that allows the clinician to image and physically characterize the stiffness of lesions. Since tissue stiffness has been associated with cancerous growth of cells as well as metastatic potential, VOCT is useful in the analysis of lesion composition. Cellular contributions to the properties of the lesion occur at resonant frequencies at and below about 60 Hz while collagen contributes at higher resonant frequencies. In BCC and AK lesions the ratio of low (cellular) and high (collagen) frequency peaks differ. The BCC lesion has a high cellular content and little collagen while the AK lesion has an approximately equal amount of cells and collagen. Enhanced VOCT images and measurements give better observations of surface roughness (hills and valleys), architecture, the ratio of cellular to collagen content and stiffness values for each component that may assist the surgeon in better characterizing skin lesions prior to and after excision. Studies are ongoing to compare VOCT results and histopathology on different lesion types to better understand the use of this technique in the clinic.

Acknowledgments

None.

Conflicts of interest

One or more of the authors may receive financial remuneration in the future from the sale of the device used in this research work.

References

1. Dewan SS. Global markets and technologies for optical coherence tomography. *Market Research Reports*. 2015.
2. Emon B, Bauer J, Jain Y, et al. Biophysics of Tumor Microenvironment and Cancer Metastasis: A Mini Review. *Comput Struct Biotechnol J*. 2018;27(16):279–287.
3. Silver FH. *Mechanosensing and Mechanochemical Transduction in Extracellular Matrix*. USA: Springer; 2006.
4. Paolino G, Donati M, Dario Didona D, et al. Histology of Non-Melanoma Skin Cancers: An Update. *Biomedicines*. 2017;5(71):5–4.
5. Apalla Z, Nashed D, Weller RB, et al. Skin Cancer: Epidemiology, Disease Burden, Pathophysiology, Diagnosis, and Therapeutic Approaches. *Dermatol Ther (Heidelberg)*. 2017;7(Suppl 1):5–19.
6. Bath-Bath-Hextall FJ, Perkins W, Bong J, et al. Interventions for basal cell carcinoma of the skin. *Cochrane Database Syst Rev*. 2007;24(1):CD003412.
7. Samani A, Bishop J, Luginbuhl C, et al. Measuring the elastic modulus of ex-vivo small tissue samples. *Phys Med Biol*. 2003;48(14):2183–2198.
8. Samani A, Zubovits J, Plewes D. Elastic moduli of normal and pathological human breast tissues: an inversion-technique-based investigation of 169 samples. *Phys Med Biol*. 2007;52:1565–1576.
9. Acerbi I, Cassereau L, Dean I, et al. Human breast cancer invasion and aggression correlates with ECM stiffening and immune cell infiltration. *Integr Biol (Camb)*. 2015;7(10):1120–1134.
10. Lin HH, Lin HK, Lin IH, et al. Mechanical phenotype of cancer cells: cell softening and loss of stiffness sensing. *Oncotarget*. 2015;6:20946–20958.
11. Lekka M. Discrimination between normal and cancerous cells using AFM. *Bionanoscience*. 2016;6:65–80.
12. Shah R, De Vore D, Pierce MG. Morphomechanics of dermis—A method for non-destructive testing and of collagenous tissues. *Skin Res Technol*. 2017;23(3):399–406.
13. Shah R, Pierce MC, Silver FH. A method for non-destructive mechanical testing of tissues and implants. *J Biomed Mater Res*. 2017;105(1):15–22.
14. Silver FH, Silver LL. Non-invasive viscoelastic behavior of human skin and decellularized dermis using vibrational OCT. *Derm Clinics & Research*. 2017;3(3):174–179.
15. Shah RG, De Vore D, Silver FH. Biomechanical analysis of decellularized dermis and skin: Initial in vivo observations using OCT and vibrational analysis. *J Biomed Mater Res A*. 2018;106(5):1421–1427.
16. Silver FH, De Vore D, Shah R. Biochemical, biophysical and mechanical characterization of decellularized dermal implants. *Material Sciences and Applications*. 2017;8:873–888.
17. Silver FH, Shah RG. Mechanical spectroscopy and imaging of skin components in vivo: Assignment of the observed moduli. *Skin Research and Technology*. 2018;25(1):47–53.
18. Silver FH, Silver LL. Use of Vibrational Optical Coherence Tomography in Dermatology. *Archives of Dermatology and Skin Care*. 2018;1(2):3–8.
19. Silver FH, Shah RG, Benedetto D, et al. Virtual biopsy and physical characterization of tissues, biofilms, implants and viscoelastic liquids using vibrational optical coherence tomography. *World J Mechanics in press*. 2019;9(1):1–16.
20. Kersten RC, Ewing Chow D, Kulwin DR, et al. Accuracy of clinical diagnosis of cutaneous eyelid lesions. *Ophthalmology*. 1997;104(3):479–484.
21. Buntin CM, Silver FH. Noninvasive measurement of rabbit aortic wall thickness using ultrasound and histological analysis. *Biomed Sci Instrum*. 1988;24:119–124.
22. Ghita MA, Caruntu C, Adrian E, et al. Reflectance confocal microscopy and dermoscopy for in vivo, non invasive skin imaging of superficial basal cell carcinoma. *Oncology Letters*. 2016;11:3019–3024.
23. Doillon CJ, Dunn MG, Bender E, et al. Collagen fiber formation in repair tissue: development of strength and toughness. *Collagen Res Rel*. 1985;5:481–492.